Enhanced mechanical properties of in-situ aluminium matrix nano composites reinforced by alumina nanoparticles

Y. Afkham[1], R. Azari Khosroshahi[1], S. Rahimpour[1], Cassra Aavani [2], D. Brabazon[3], R. Taherzadeh Mousavian[1,*]

1: Faculty of Materials Engineering, Sahand University of Technology, Tabriz, Iran

2: Department of Mechanical Engineering, Payame Noor University (PNU), Tehran, Iran

3: Advanced Processing Technology Research Centre, School of Mechanical & Manufacturing Engineering, Dublin City University, Dublin 9, Ireland

Email: rtaher1898@gmail.com, r_taherzadeh@sut.ac.ir

Tel: +98 919 9591160

Abstract

In-situ fabrication of metal matrix nano composites has various advantages such as the formation of clean particle-metal interface with strong bonding. In this study, three types of metal oxides powders (commercial TiO_2, commercial ZnO, and recycled Pyrex) were used to inject into the pure aluminium melt to fabricate in-situ aluminium matrix nano composites via liquid-state stir casting at 850 °C followed by a hot rolling process. SEM and FESEM microstructural characterizations, as well as EDAX analysis, were used to show if in-situ reactions occurred between molten aluminium and metal oxides to form nano alumina particles as the reinforcement. Tensile and microhardness tests were also applied on the rolled nano composites to identify the effect of metal oxide type and amount on the mechanical properties. It was found that using recycled Pyrex crushed powders led to the formation of a uniform distribution of alumina nanoparticles, while fine-micron ZnO and especially TiO_2 powders could not be uniformly distributed into the melt for complete reaction occurrence.

Keywords: Aluminium nano composite; In-situ method; Liquid-state stirring; Mechanical properties.

1. Introduction

Recently, metal matrix composites (MMCs) have drawn a great attention for their incomparable properties and structures [1-3]. MMCs play a crucial role in the automotive, aerospace, and other industries because of the typically low cost of their reinforcements and the well-developed production methods [4]. Aluminium alloys have been gaining greater attention as the matrix of MMCs due to their unique physical and mechanical properties [5-9]. Much research has been conducted to improve the structural and mechanical properties of the aluminium matrix nano composites (AMNCs) by the addition of submicron and nano-sized particles as reinforcement [10-16].

Traditionally, reinforcements are added to a metallic matrix by an ex-situ method [17] which provides a lower limit on the size of the reinforcing particles because of poor wettability between the reinforcement and the matrix due to increased surface area and the presence of surface contamination on the reinforcements [18, 19]. To overcome these drawbacks, a method has been developed, in which reinforcements are established in the matrix by one or more chemical reactions, termed in-situ method [20]. In-situ synthesizing can be obtained by many approaches such as reactive hot pressing (RHP), combustion synthesis or direct metal/metal oxidation (DIMOX) [18, 21-23]. DIMOX process is based on a reaction between the pure metal and metal oxides, which is the most promising route for fabricating in-situ reinforcements because of its simplicity, high-productivity and ease of control of the composite structure. Alumina, in particular, can be formed as reinforcement of the matrix during this method [24-27]. The general reaction of in-situ AMNCs can be represented as [28]:

$$2xAl + 3M_yO_x \rightarrow 3yM + xAl_2O_3 \quad (1)$$

Various metal oxides can be used to produce in-situ AMNCs, such as zinc oxide [20]. Kobashi and Choh [29] added zinc oxide powder to the molten aluminium. Subsequent work was accomplished by Chen and Sun [28], Yu et al. [30], Durai et al. [31], and Tavoosi et al. [32] in which zinc oxide was used to produce in-situ AMNCs. Their results showed low reactivity between zinc oxide and molten aluminium due to the zinc oxide fine particle size and its poor wettability by aluminium. Maleki et al. [20] overcame this problem by developing a new method named activated powder injection (API), in which Al and ZnO powders were mixed and milled in a ball mill to activate the ZnO powders to react with the melt in a shorter time and at a lower temperature. Other advantages of this method are deagglomeration of the metal oxide particles during milling in a matrix of aluminium and increased wettability during injection into the melt due to the presence of an aluminium layer. Many other metal oxides have also been used as the source of oxygen to react with Al and form fine Al_2O_3 reinforcing particles in the aluminium matrix such as NiO, TiO_2, Fe_2O_3, CuO, and ZnO [33-38].

In this study, three types of oxide powders were used to study the fabrication of in-situ AMNCs. TiO_2 and ZnO oxides were purchased as commercial powders. In addition, in order to show if recycled oxides can be used as a promising source for fabrication of low-cost in-situ AMNCs, Pyrex crushed powders were also used as the third type of oxide particles. In order to deagglomerate the metal oxide powders from their initial condition, they were ball-milled with pure aluminium powders before casting. Microstructural and mechanical properties of the final composites were compared to develop the DIMOX method for preparation of valuable in-situ AMNCs materials.

2. Materials and Methods

An aluminium bar with purity of 99.8% (from Iralco Co., Iran) was used as the matrix. Also, aluminium powder (purity of 99.8%, from Khorasan Powder Metallurgy Co., Iran) with an average particle size below 20 μm, TiO_2, and ZnO oxide powders (both from Millennium Co., China) were also used in the present study. Recycled Pyrex powders (sodium borosilicate glass) with the chemical composition as shown in Table 1 [39] were obtained by ball milling (using a Sepahan 84D planetary ball mill) of useless Pyrex materials. Figs. 1a and 1b show the morphology of crushed Pyrex powders after 5 and 30 min ball milling, respectively. In addition, Fig. 1c showed the as-received TiO_2 and ZnO powders. Fig. 1a shows that large sized Pyrex powders with sharp edges were still present after 5 min milling, requiring a higher milling time for crushing. Fig. 1b shows that ball milling from 5 to 30 min with four 20 mm-alumina-balls with the rotation speed of 550 rpm under air atmosphere can highly reduce the average particle size of crushed powders with a higher sphericity in respect to 5 min milled Pyrex powders without considerable agglomeration. In should be noted that before ball milling, a hammer was used for crashing of large sized Pyrex parts. Considerable agglomeration can also be seen for both the TiO_2 and ZnO as-received powders (see Fig. 1c).

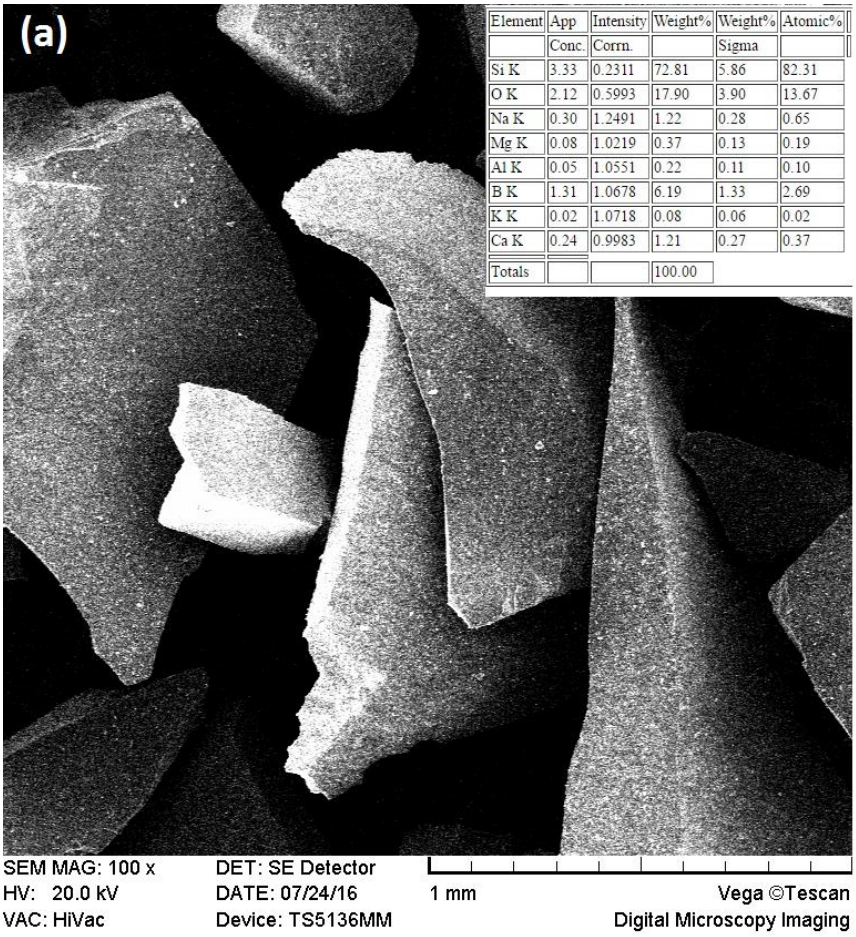

Element	App Conc.	Intensity Corrn.	Weight%	Weight% Sigma	Atomic%
Si K	3.33	0.2311	72.81	5.86	82.31
O K	2.12	0.5993	17.90	3.90	13.67
Na K	0.30	1.2491	1.22	0.28	0.65
Mg K	0.08	1.0219	0.37	0.13	0.19
Al K	0.05	1.0551	0.22	0.11	0.10
B K	1.31	1.0678	6.19	1.33	2.69
K K	0.02	1.0718	0.08	0.06	0.02
Ca K	0.24	0.9983	1.21	0.27	0.37
Totals			100.00		

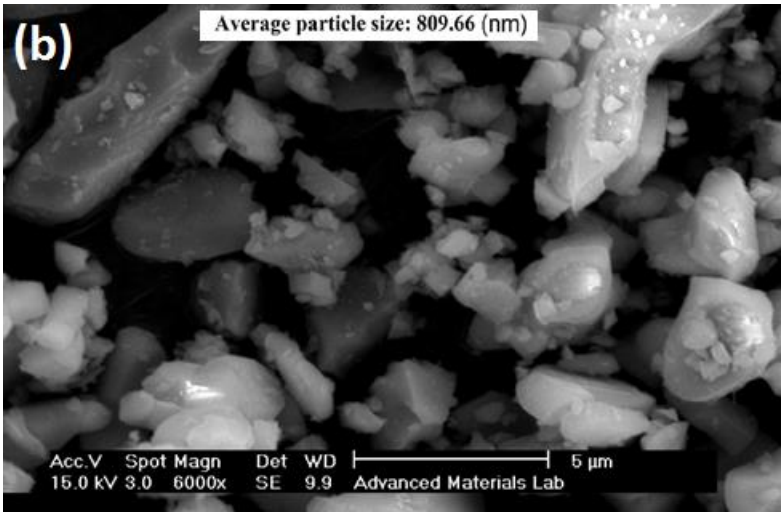

Fig. 1.The SEM morphology of crushed Pyrex powders after, (a) 5 min, (b) 30 min and (c) illustration of as received TiO_2, and ZnO powders.

Table 1: Chemical composition of Pyrex 7740 glass (Mol%)

SiO_2	B_2O_3	Na_2O	Al_2O_3	K_2O	MgO	CaO
80.8	12	4.2	2	0.6	0.2	0.2

In order to deagglomerate the fine oxide particles, 15 g of each oxide powders (ZnO, TiO_2, and 30-min crushed Pyrex) were separately added to 15 g of pure Al powder for ball milling process for 2 hours at a constant milling speed of 250 rpm under argon (99.99 % purity) atmosphere. The ball to powder weight ratio of 3:1 and the alumina balls (with 20 and 10 mm diameters) were used. To prevent the occurrence of severing adhesion of the mixture powder particles to balls and mill walls, stearic acid at 1 wt.% was used as a process control agent (PCA). After milling process, to remove impurities, surface contaminations, and absorbed water molecules on the surface of the particles, as-milled powders were pre-heated under argon atmosphere for 2 hours at 400 ˚C using ATBIN heat treatment furnace just before liquid-state stir casting process.

Four samples were prepared according to the Table 2. A bottom-pouring stir casting system was used for the casting process [39-41]. For this purpose, 500 g of the pure aluminium bar was placed and heated to 850˚C. The mixture of aluminium melt and the milled powders was stirred for 5 minutes, after 1-min completion of powder particles addition (total 6 min), to obtain better contact between oxide powders and aluminium melt. This resulted in the formation of a uniform distribution of alumina-reinforcing nanoparticles. These alumina nanoparticles can be obtained due to the following chemical reactions with molten aluminium at 850 °C:

Pyrex 7740 glass:

- $4Al(l) + 3SiO_2(s) \rightarrow 3Si(s) + 2Al_2O_3(s)$, $\Delta H°_{298\ K}$ = -681.4 kJ/mol (2)
- $2Al(l) + B_2O_3(s) \rightarrow 2B(s) + Al_2O_3(s)$, $\Delta H°_{298\ K}$ = -421.7 kJ/mol (3)
- $2Al(l) + 3Na_2O(s) \rightarrow 6Na(l) + Al_2O_3(s)$, $\Delta H°_{298\ K}$ = -427.7 kJ/mol (4)
- $2Al(l) + 3K_2O(s) \rightarrow 6K(l) + Al_2O_3(s)$, $\Delta H°_{298\ K}$ = -586.19 kJ/mol (5)
- $2Al(l) + 3MgO(s) \rightarrow 3Mg(l) + Al_2O_3(s)$, $\Delta H°_{298\ K}$ = 129.7 kJ/mol (6)
- $2Al(l) + 3CaO(s) \rightarrow 3Ca(l) + Al_2O_3(s)$, $\Delta H°_{298\ K}$ = 229.3 kJ/mol (7)

$\Delta H°_{298\ K}$ (total)= -621.61 kJ/mol (8)

ZnO: $2Al(l) + 3ZnO(s) \rightarrow 3Zn(s) + Al_2O_3(s)$, $\Delta H°_{298\ K}$ = -631.7 kJ/mol (9)

TiO_2: $4Al(l) + 3TiO_2(s0 \rightarrow 3Ti(s) + 2Al_2O_3(s)$, $\Delta H°_{298\ K}$ = -516.4 kJ/mol (10)

Our previous studies have indicated that metal oxide particles, which are brittle in nature, are covered by ductile aluminium powders [42-44]. Aluminium powders cover the metal oxide particles and aid the balls collisions to make the oxide powders more deagglomerated. The presence of aluminium powders can also lead to a better distribution of activated oxide particles in the melt, resulting in their gradual reaction with the molten aluminium. The other details of casting equipment and process were reported elsewhere [45].

Table 2: The composition of prepared samples.

Samples	Composite slurry mixture
S_1	Al-4wt% Pyrex
S_2	Al-6wt% Pyrex
S_3	Al-6wt% TiO_2
S_4	Al-6wt% ZnO

After the casting process, hot rolling as previously detailed [46, 47]. Microstructural characterizations of composite samples were performed using a scanning electron microscopy (SEM, Cam Scan MV2300) and a field emission scanning electron microscopy (FESEM-Mira Tescan) equipped with EDAX analysis.The phase composition of the samples after ball milling were characterized using X-ray diffraction (XRD, Bruker's D8 advance system, Germany) with Cu Kα (λ=0.15405 nm) radiation source. To investigate the mechanical properties, tensile test (three times) and micro-hardness tests (on ten points) were carried out by DY-26 model tensile/pressure system with a compressing capacity of 10 tones according ASTM E384 standard (The standard of micro-hardness test). Dimensions of the tensile test sample were also reported in our previous studies [45].

3- Results and Discussion

As mentioned, in order to fabricate an in-situ AMNC reinforced by alumina nanoparticles, Pyrex, TiO_2, and ZnO powders were ball-milled with the aluminium powders and then injected into the aluminium melt at 850 °C for the occurrence of exothermic reactions during 6 min stirring. Fig. 2 shows the results of the XRD analysis of the samples. As can be seen in Fig. 2a, Pyrex has completely reacted with aluminium and there is no evidence of remained unreacted oxides. It can be seen that incorporation of 6 wt. % of Pyrex powders resulted in the formation of alumina phase via reactions (2-7). According to the Eq. (10), a complete reaction between

aluminium and TiO_2 was supposed to take place with the formation of alumina. Nevertheless, uncompleted reaction occurred and remains of unreacted TiO_2 can be observed in Fig. 2b, while ZnO had further involved in exothermic reactions and a higher rate of alumina was created (Fig. 2c). Previous literature [47] has indicated that this temperature is high enough for completion of the exothermic reactions for these three metal oxide powders in the molten aluminium Hence, it can be concluded that in spite of high temperature and six-minute mixing, considerable amount of agglomeration can result in occurrence of uncompleted reactions. Figs. (3-6) show the SEM/EDAX analysis results of as-cast composites before the rolling process. Fig. 3 is related to FESEM microstructure of sample S_1 after casting and solidification, in which 4 wt. % Pyrex crushed powders were entered with the aid of ball milling with aluminium powders. In the low-magnification image of Fig. 3 (left-hand side), the grain-boundaries are evident. This occurrence indicated that Eq. 2 took place at 850 °C because of the reaction between molten aluminium with Pyrex powders to form fresh residual silicon during stirring, and due to the very low solubility of silicon in molten aluminium [48], eutectic silicon phase forms at the grain boundaries after solidification. This low-magnification image (Fig. 3) also shows the presence of some particles mostly below 5 µm. In order to find out the results of reaction between Pyrex powders with molten aluminium, high-magnification FESEM image was shown on the right-hand side of Fig. 3. It can be seen that AMNC reinforced by a semi-ideal distribution of nano alumina particles with the particle size even lower than 30 nm was fabricated as the product of Eqs. (2-7). However, it can be seen that agglomeration also occurred by adhesion of nanoparticles to each other during stirring or by being pushed during solidification. It is very difficult to distribute as-received nano ceramic particles by an ex-situ casting method in a

similar manner to what shown in Fig. 3 for the in-situ method applied in this work. This highlights the beneficial effects of the in-situ methodology. Instead of expensive nano alumina particles, low-cost recycled Pyrex originated powders were capable of providing this.

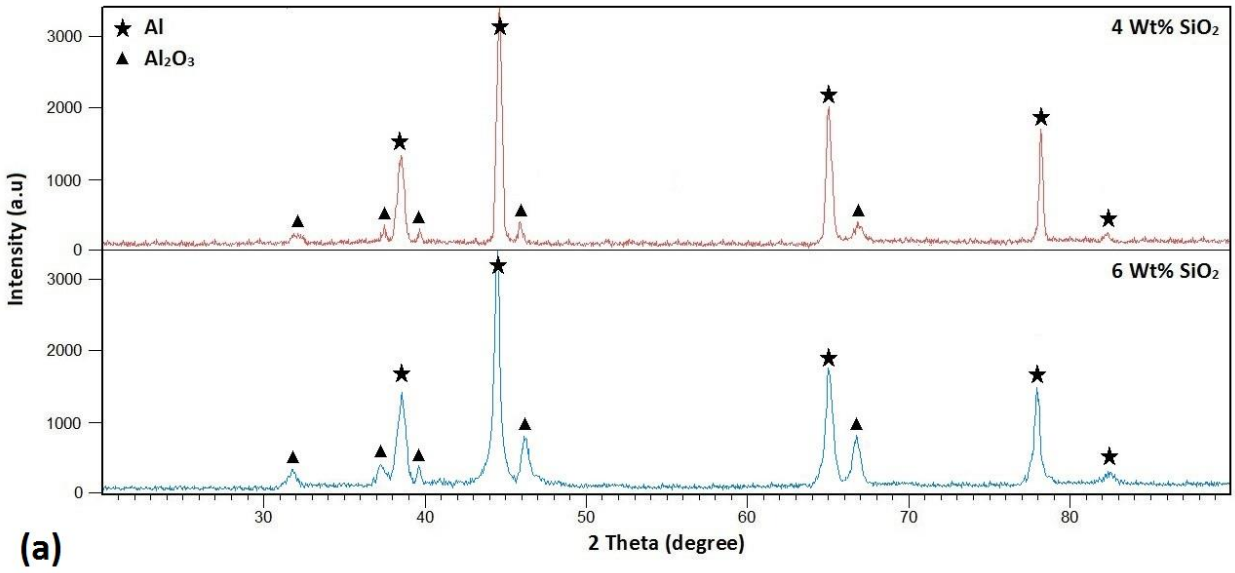

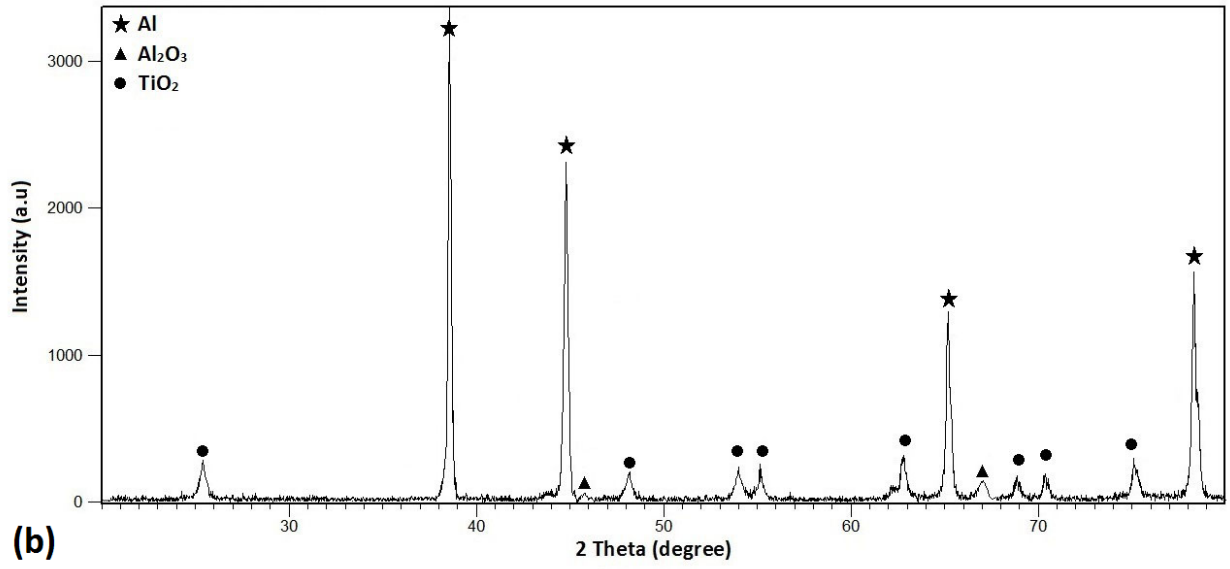

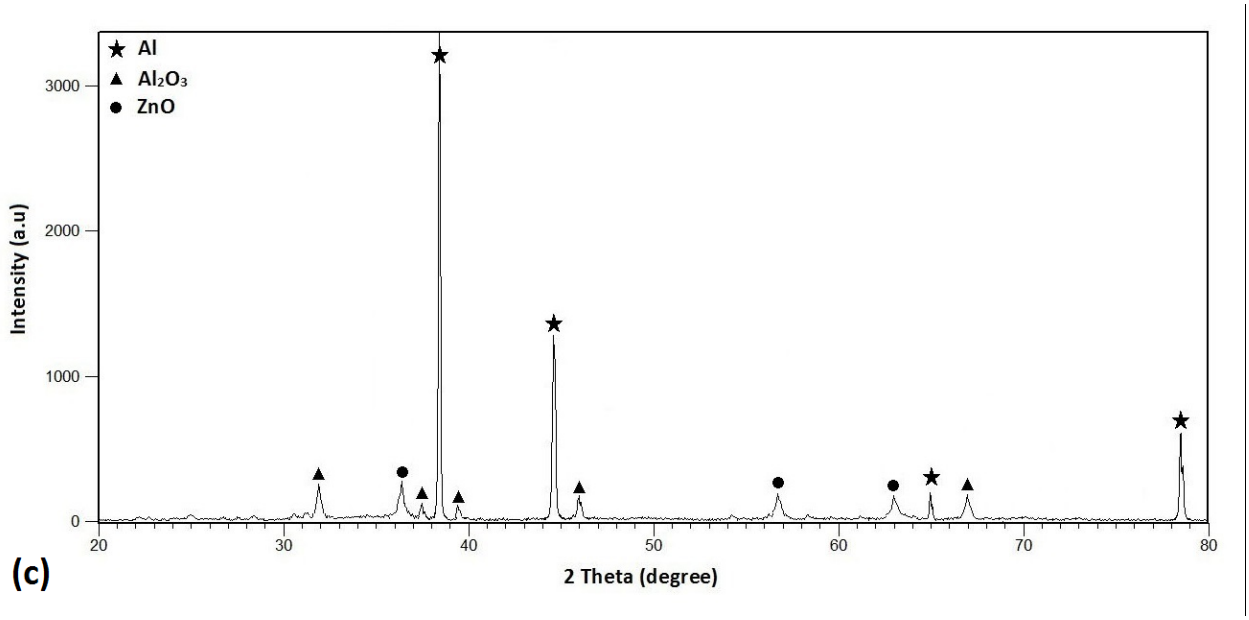

Fig. 2. XRD pattern of the samples (a) S_1 and S_2, (b) S_3 and (c) S_4 after casting process.

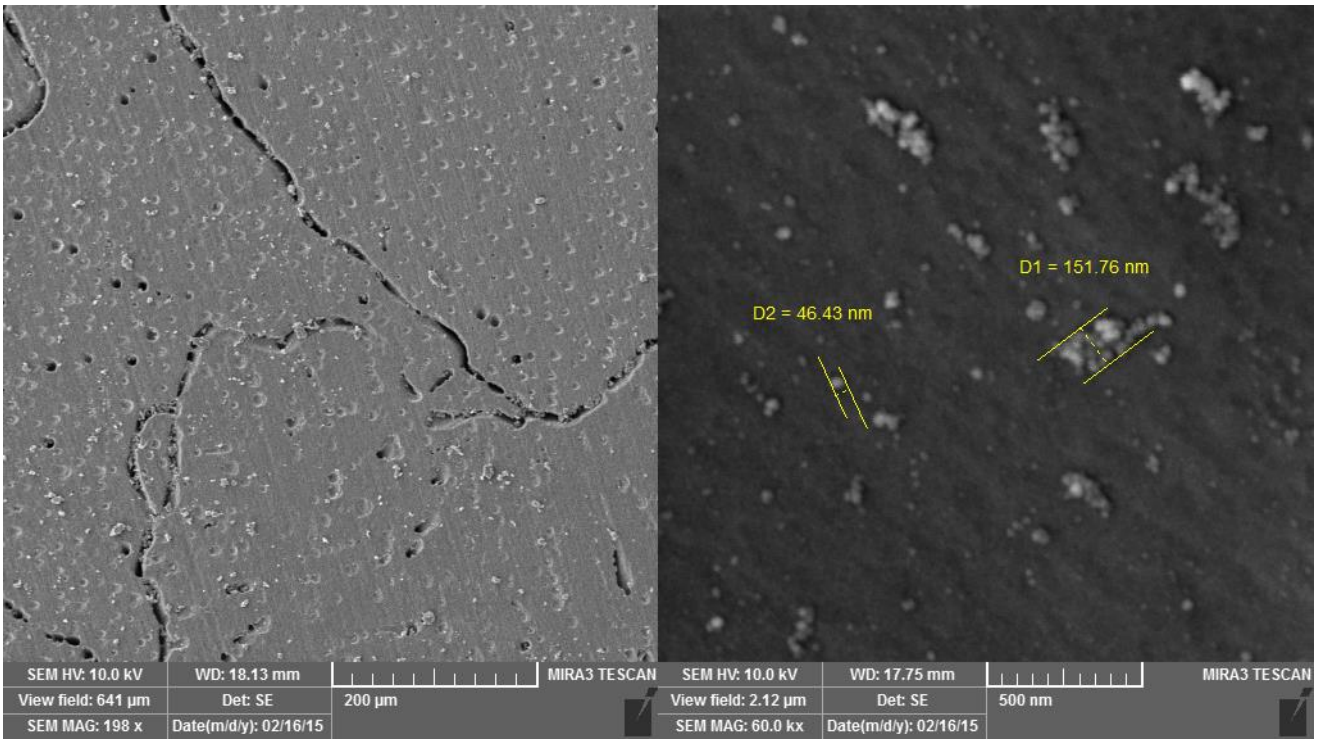

Fig. 3. The FESEM morphology of sample S_1(Al-4wt% Pyrex) after casting and solidification.

Fig. 4 shows the microstructure of sample S_2, in which 6 wt.% Pyrex powders were injected into the melt by the aid of milling with aluminium powders. From the low-magnification image, no

considerable difference can be seen between the samples S_1 and S_2. However, from the high-magnification image, it seems that the number of reinforcing phases is considerably higher than that of sample S_1. A great number of nanoparticles can be observed in the microstructure as a higher value of oxide powders was injected to form a higher value of nano alumina particles. Although, the number of nanoparticles for sample S_2 was higher than that of sample S_1, however, it can be seen that no extra agglomeration occurred with respect to the sample S_1. EDAX analysis on the area marked by red colored X indicated the presence of a very low amount of silicon and a considerable amount of aluminium and oxygen, indicating the transferring of oxygen from SiO_2 to Al and formation of alumina.

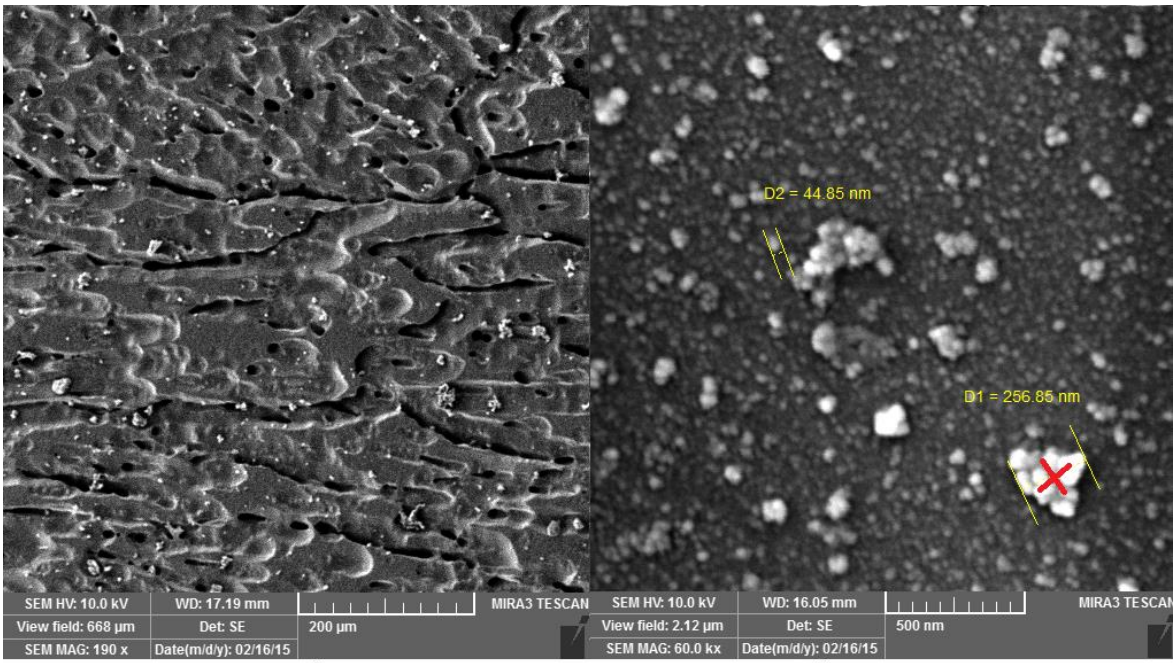

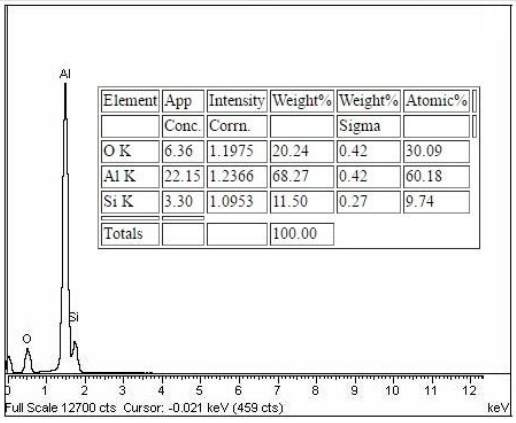

Element	App	Intensity	Weight%	Weight%	Atomic%
	Conc.	Corrn.		Sigma	
O K	6.36	1.1975	20.24	0.42	30.09
Al K	22.15	1.2366	68.27	0.42	60.18
Si K	3.30	1.0953	11.50	0.27	9.74
Totals			100.00		

Fig. 4. The FESEM morphology of sample S_2 (Al-6 wt.% Pyrex) after casting and solidification.

Fig. 5 shows the as-cast microstructure of sample S_3, in which fine TiO_2 powders that had been milled by aluminium powders were injected into the melt of pure aluminium. It can be seen that very large-sized agglomerated TiO_2 milled powders were remained after stirring. These powders were unbraided after stirring. Lower enthalpy of reaction 10, compared with that of reaction 8, and severe agglomeration of TiO_2 powders (see Fig. 1c) were the two possible causes of TiO_2 powders for being unbraided. In addition, many other unbraided TiO_2 particles between 5-20 µm can be seen in the as-cast microstructure of sample S_3. The trace of Ti and O

elements can be seen in EDAX analysis of Fig. 5, indicating that the red-colored marked area shows the presence of TiO_2 powders. It is important to note that high-magnification FESEM microstructure of Fig. 5 showed the distribution of nano alumina particles even in the range of 30 nm, indicating that reaction (10) took place when fine single TiO_2 powders were exposed to the melt for the preparation of nano alumina particles.

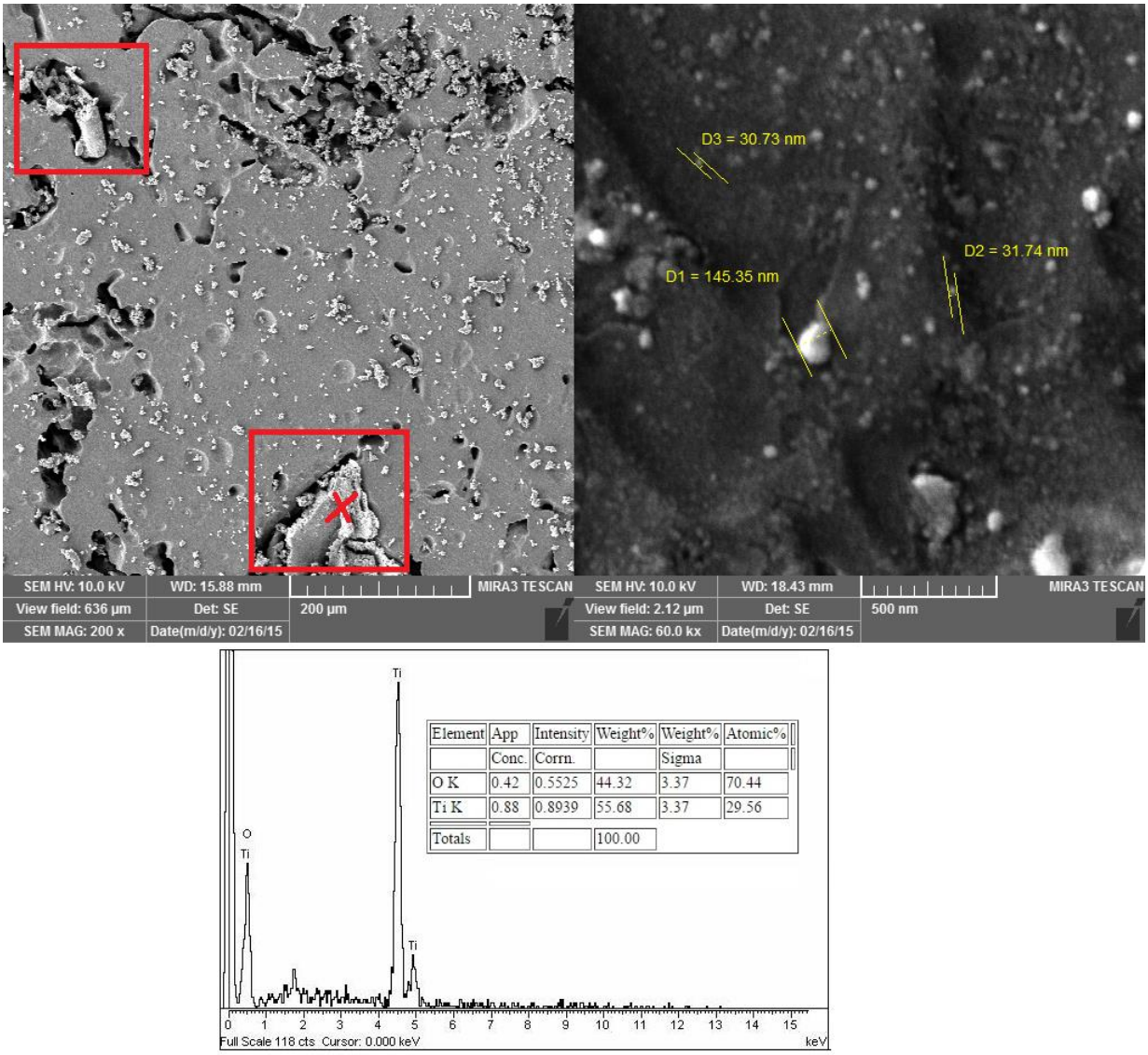

Fig. 5. The FESEM morphology of sample S_3 (Al-6wt% TiO_2) after casting and solidification.

The last as-cast microstructure is shown in Fig. 6 that is related to the sample S_4. For this sample, ZnO powders were used as a metal oxide for exothermic reaction with molten aluminium. Similar to the previous samples, many submicron particles as well as large-sized unbraided ZnO enriched clusters (shown by red-colored rectangles) were revealed on the low-magnification structure. On the other hand, the high-magnification image also showed the reaction occurrence that led to the fabrication of alumina nanoparticles that were distributed uniformly in some zones, while extreme agglomeration also occurred. EDAX analysis shows the trace of oxygen and aluminium enriched zones on the red-colored marked area. Therefore, it can be concluded that these agglomerated nano alumina particles adhered to each other during stirring at 850 °C after reaction occurrence and/or after solidification by pushing ahead of solidification front.

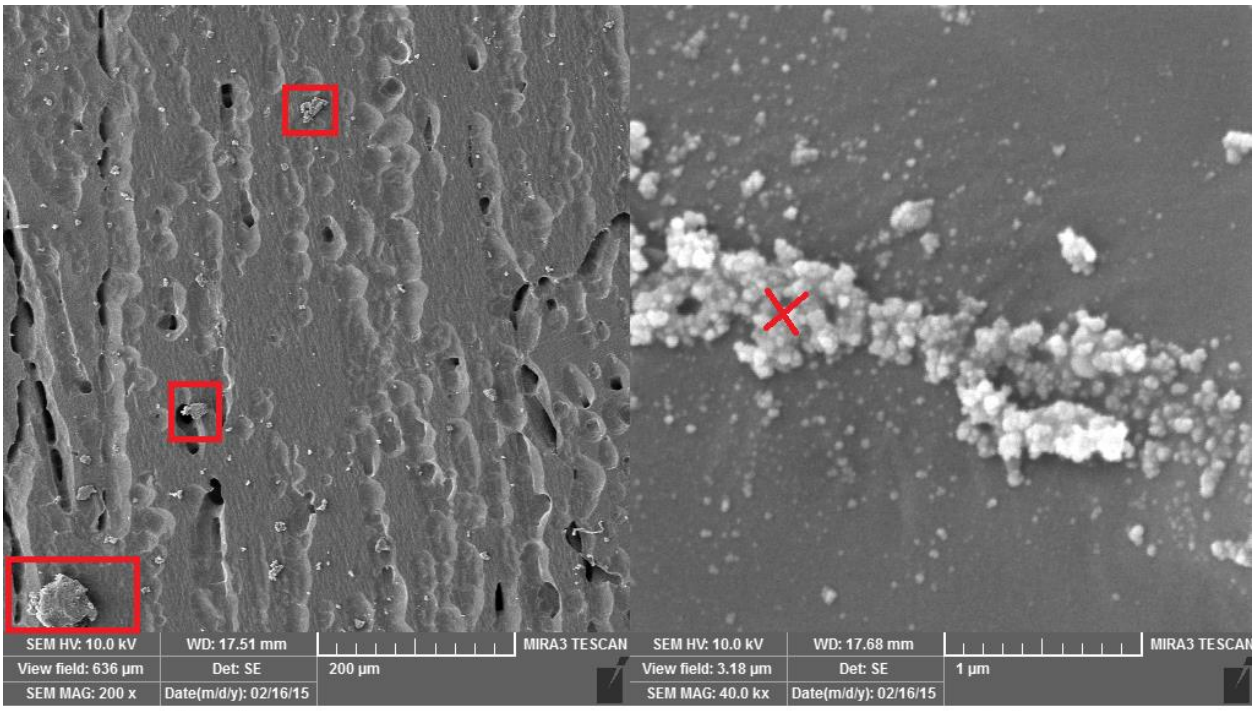

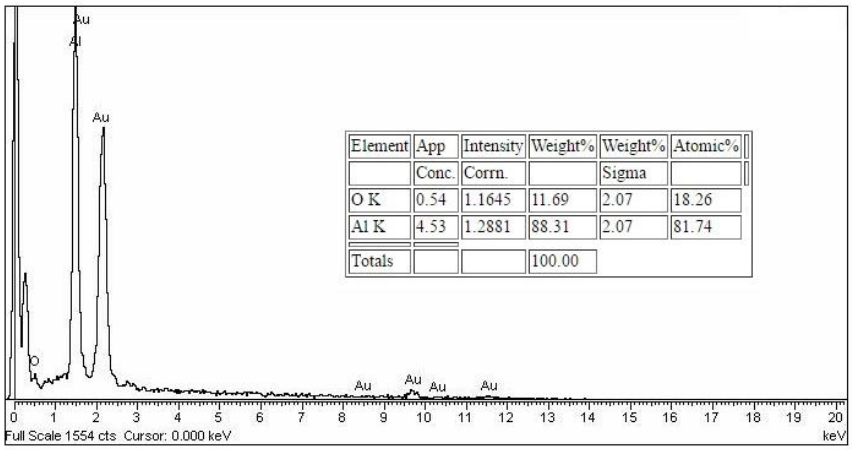

Element	App Conc.	Intensity Corrn.	Weight%	Weight% Sigma	Atomic%
O K	0.54	1.1645	11.69	2.07	18.26
Al K	4.53	1.2881	88.31	2.07	81.74
Totals			100.00		

Fig. 6. The FESEM morphology of sample S_4 (Al-6wt% ZnO) after casting and solidification.

As-cast in-situ composites cannot be used in industry due to the presence of various kinds of porosities and solidification shrinkages as well as the occurrence of fine particle agglomeration. In order to increase their mechanical properties to become applicable, secondary thermomechanical processes can be used to overcome the mentioned drawbacks. The hot-rolling process was applied on the fabricated as-cast composites and Fig. 7 shows the SEM microstructures of the rolled samples. Figs. 7a and 7b are related to the samples S_1 and S_2,

respectively. It can be seen that many submicron-sized alumina particles were distributed in the matrix, indicating that reaction (8) did not completely lead to the formation of nanoparticles. Fig. 1b indicated that the average particle size of Pyrex crushed powders after 30-min ball milling was about 800 nm, and therefore, the formation of submicron-sized alumina particles after reaction occurrence is also expected. Therefore, multi-modal sized alumina particles were prepared and distributed in the matrix of aluminium alloy. No porosity was also revealed for these two samples and just the number of alumina particles for the sample S_2 was considerably higher than that of sample S_1.

Figs. 7c and 7d showed unexpected results after the rolling process. Some cracks were revealed, in particular for the sample S_3, indicating that severe agglomeration of metal oxide particles and possible formation of brittle intermetallic compounds in Al-Ti and Al-Zn alloys might lead to local fracture and crack formation during the rolling process.

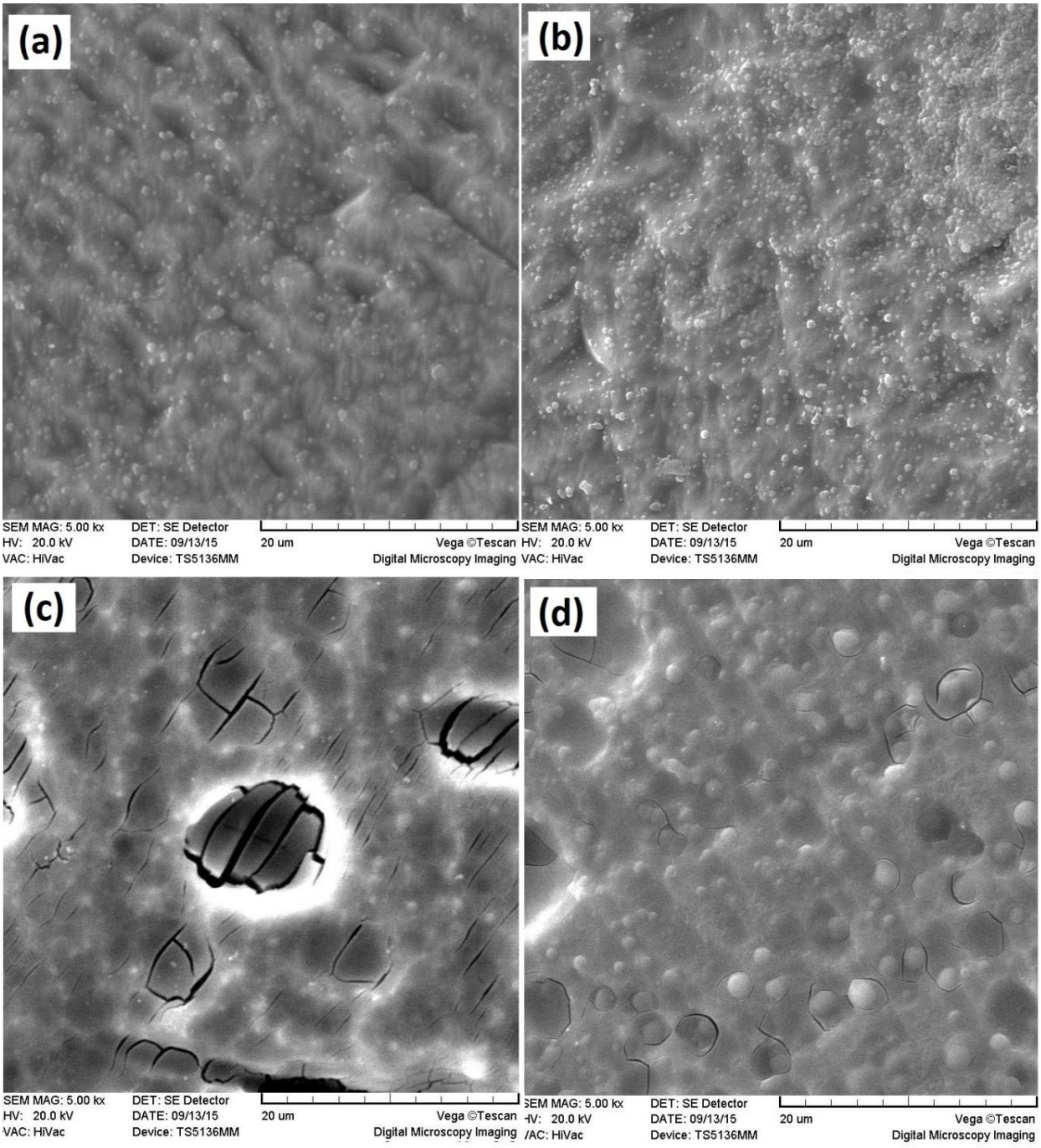

Fig. 7. The SEM morphology of rolled samples, (a) S_1, (b) S_2, (c) S_3, and (d) S_4.

Table 3 summarizes the mechanical properties of the rolled samples after tensile test for three times and microhardness measurements. In order to find the effect of in-situ composite fabrication, pure aluminium ingot after stir casting at 850 °C was exposed to the hot-rolling.

Afterward, the main samples were tested. Some important points can be drawn from this Table. Firstly, the most ductile reinforced sample was S_1, in which 4 wt. % Pyrex powders were injected. For this sample, a 52 % improvement in the UTS and YS occurred with respect to the pure aluminium, which was expected as a suitable nanoparticle distribution was obtained (see Fig. 3). Secondly, sample S_2 with an injection of 6 wt.% Pyrex powders showed the highest UTS and YS values, 59 and 66 % higher than that of pure aluminium, respectively, while its ductility is lower than that of sample S_1. Thirdly, sample S_3 has the minimum UTS, YS, and ductility with respect to all the composite samples. The formation of many cracks and the severe agglomeration and unbraided clusters were effective on the reducing the mechanical properties. Severe agglomeration of TiO_2 powders is the main reason that even ball milling seems not to be completely effective for deagglomeration occurrence. Fourthly, the tensile properties of sample S_4 was lower than that of sample S_1, indicating that morphology of metal oxide powders (to be agglomerated or single) is more important than the amount of injected metal oxide and the reaction enthalpy between metal oxide and aluminium as reaction (9) has a higher enthalpy than reaction (8). Fifthly, composite fabrication, as expected, increased the hardness and the highest value of hardness was obtained for the sample S_2, in which more than 65 % increase was obtained.

Table 3: The mechanical properties of the samples after the rolling process.

Sample	UTS (MPa)	Ductility (%)	YS (MPa)	Hardness (HV)	Standard deviation for Hardness measurements (HV)
Pure rolled aluminium	81^{+3}_{-2}	$39^{+0.7}_{-0.8}$	44^{+3}_{-2}	49	3
S_1 (Al-4 wt. % SiO_2)	123^{+7}_{-5}	$29^{+0.4}_{-0.3}$	67^{+5}_{-3}	72	6
S_2 (Al-6 wt. % SiO_2)	129^{+9}_{-6}	$22^{+1.2}_{-0.4}$	73^{+4}_{-7}	81	9
S_3 (Al-6 wt. % TiO_2)	104^{+4}_{-7}	$7^{+0.2}_{-0.3}$	52^{+2}_{-5}	67	7
S_4 (Al- 6 wt. % ZnO)	114^{+5}_{-4}	$13^{+0.5}_{-0.7}$	58^{+6}_{-2}	74	8

In order to have a better understanding of the mechanical properties and, in particular, ductility, SEM fracture surface is helpful. Figs. 8a and b show the ductile nature of samples S_2 and especially, sample S_1, in which cup and cone morphologies were obtained. However, the trace of particle agglomeration was shown in Fig. 8b for the sample S_2, which was expectable. In contrast, Figs. 8c and d showed the brittle nature of samples S_3 and S_4 due to the negative effect of large clusters for these samples.

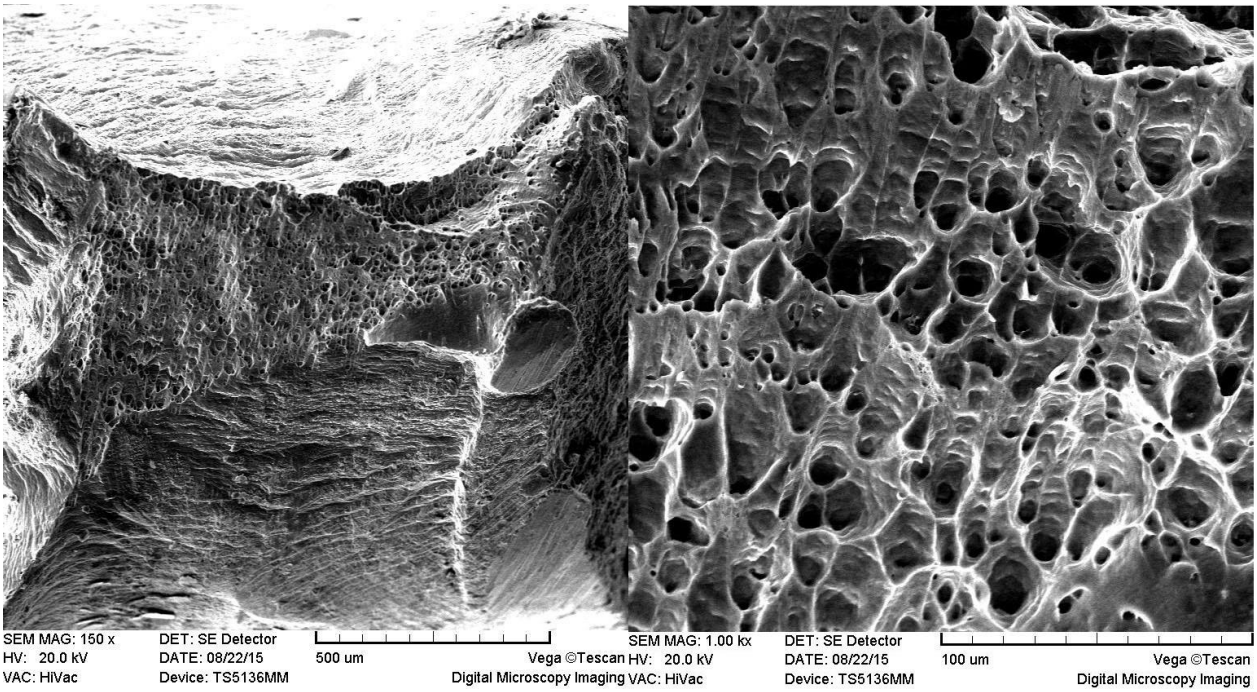

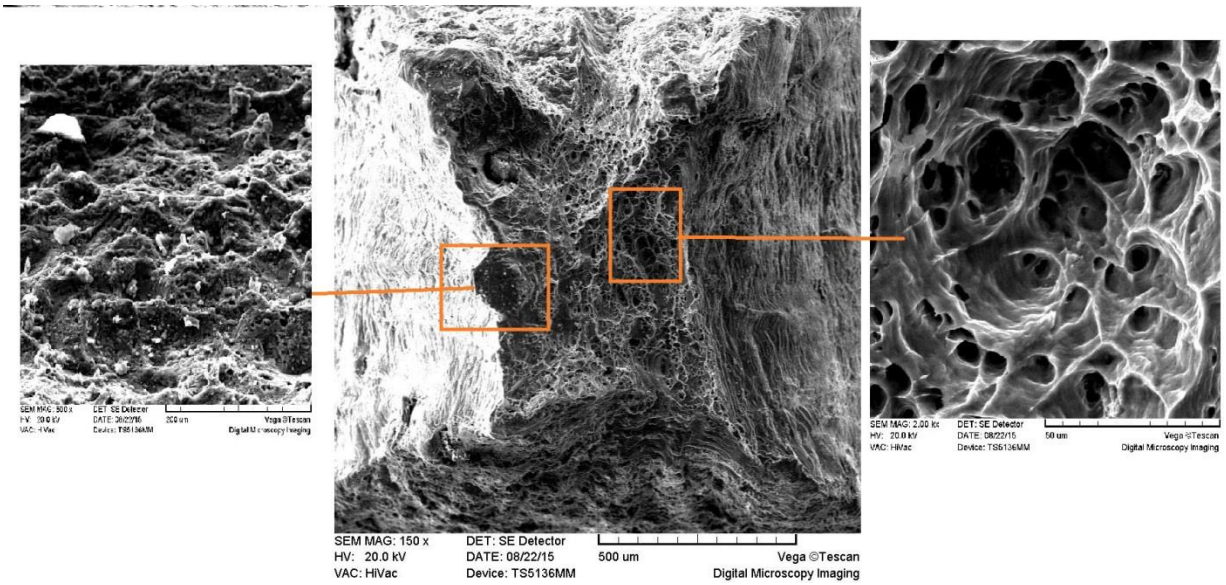
SEM MAG: 150 x
HV: 20.0 kV
VAC: HiVac
DET: SE Detector
DATE: 08/22/15
Device: TS5136MM
500 um
Vega ©Tescan
Digital Microscopy Imaging

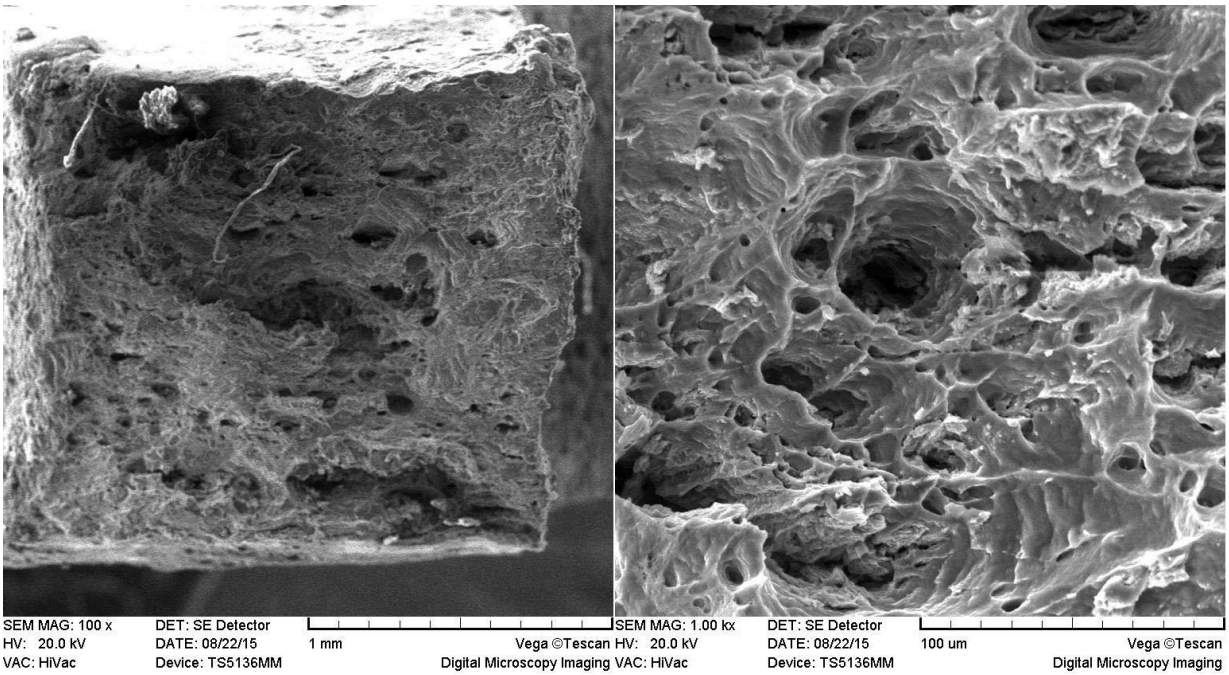
SEM MAG: 100 x
HV: 20.0 kV
VAC: HiVac
DET: SE Detector
DATE: 08/22/15
Device: TS5136MM
1 mm
Vega ©Tescan
Digital Microscopy Imaging
SEM MAG: 1.00 kx
HV: 20.0 kV
VAC: HiVac
DET: SE Detector
DATE: 08/22/15
Device: TS5136MM
100 um
Vega ©Tescan
Digital Microscopy Imaging

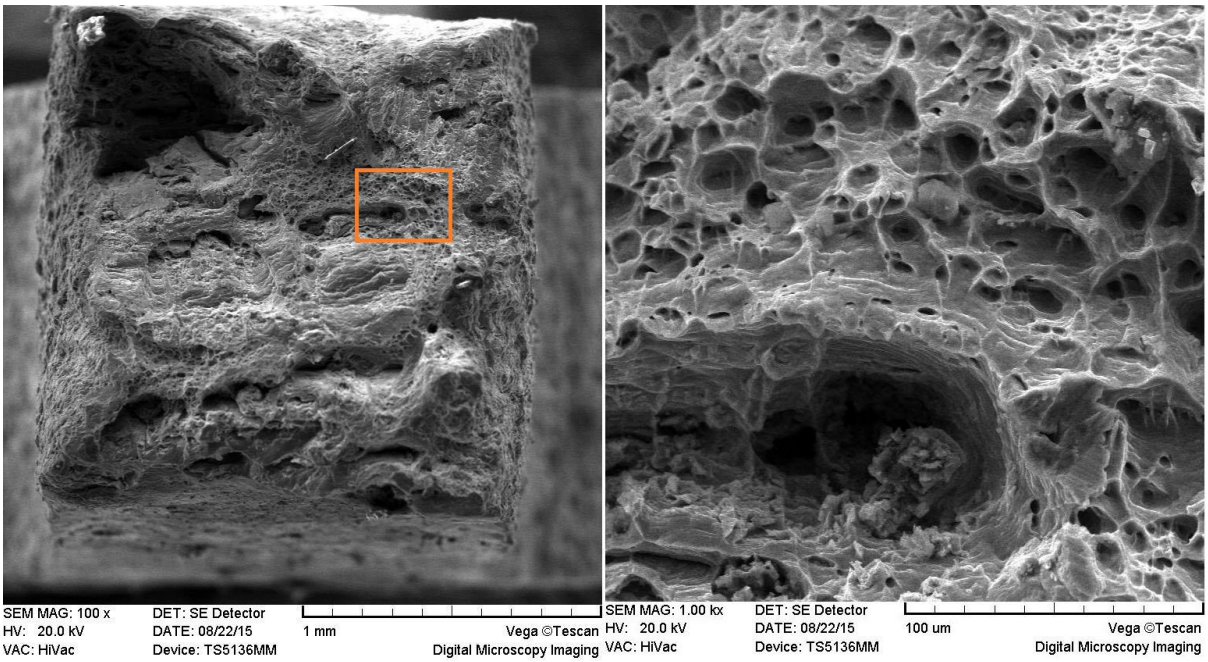

Fig. 8. The SEM fracture surface of rolled samples, (a) S_1, (b) S_2, (c) S_3, and (d) S_4.

4- Conclusions

In this study, in-situ aluminium matrix nanocomposites were fabricated via the in-situ stir casting method followed by hot rolling. For improving the agglomerating condition of metal oxide powders, ball milling process was used to mill three types of metal oxide powders with aluminium particles. From the experimental results the following conclusions can be drawn:

1: The morphology and condition of metal oxide powders for reaction with aluminium melt is the most important issue for obtaining a suitable distribution of alumina nanoparticles.

2: By using submicron metal oxide powders, nano alumina particles can be obtained as a result of exothermic reactions. Incorporation of Pyrex, ZnO, and TiO_2 powders led to formation of a higher amount of alumina phase, respectively, since the rate of agglomeration has a serious impact on occurrence of complete reactions, in spite of high temperature and mixing for 6 min.

3: By using ball milling process, waste Pyrex glass can be converted to amorphous powders with a varying size ranges from nano to fine micron ranges. It was observed that these powders with low agglomeration could be uniformly distributed in the matrix.

4: Unbraided clusters of ZnO and especially TiO_2were revealed in as-cast microstructures. ZnO and, in particular, TiO_2 powders were present in an agglomerated form. These clusters were the main reason for the formation of cracks in the microstructure after hot-rolling.

5: Mechanical properties of the composites indicated that higher injection of Pyrex powders from 4 to 6 wt. % will lead to an increase in the hardness, UTS, and YS, while ductility reduction was observed. It was finally shown that as-received ZnO and TiO_2 powder injection did not provide as effective an improvement in mechanical properties with respect to the usage of lower cost Pyrex derived powders.

References

[1] I. Ibrahim, F. Mohamed, and E. Lavernia, "Particulate reinforced metal matrix composites—a review," Journal of materials science, vol. 26, pp. 1137-1156, 1991.

[2] Q. Zhanh, G. Wu, and L. Jiang, "Tensile deformation behavior of a sub-micrometer Al2O3/6061Al composite [J]," Materials Science and Engineering A, vol. 483, pp. 281-284, 2008.

[3] B. Prabhu, C. Suryanarayana, L. An, and R. Vaidyanathan, "Synthesis and characterization of high volume fraction Al–Al 2 O 3 nanocomposite powders by high-energy milling," Materials Science and Engineering: A, vol. 425, pp. 192-200, 2006.

[4] A. F. Boostani, S. Yazdani, R. T. Mousavian, S. Tahamtan, R. A. Khosroshahi, D. Wei, et al., "Strengthening mechanisms of graphene sheets in aluminium matrix nanocomposites," Materials & Design, vol. 88, pp. 983-989, 2015.

[5] A. F. Boostani, S. Tahamtan, Z. Jiang, D. Wei, S. Yazdani, R. A. Khosroshahi, et al., "Enhanced tensile properties of aluminium matrix composites reinforced with graphene encapsulated SiC nanoparticles," Composites Part A: Applied Science and Manufacturing, vol. 68, pp. 155-163, 2015.

[6] H. Ahamed and V. Senthilkumar, "Experimental investigation on newly developed ultrafine-grained aluminium based nano-composites with improved mechanical properties," Materials & Design, vol. 37, pp. 182-192, 2012.

[7] A. F. Boostani, R. T. Mousavian, S. Tahamtan, S. Yazdani, R. A. Khosroshahi, D. Wei, et al., "Solvothermal-assisted graphene encapsulation of SiC nanoparticles: A new horizon toward toughening aluminium matrix nanocomposites," Materials Science and Engineering: A, vol. 653, pp. 99-107, 2016.

[8] A. F. Boostani, R. T. Mousavian, S. Tahamtan, S. Yazdani, R. A. Khosroshahi, D. Wei, et al., "Graphene sheets encapsulating SiC nanoparticles: a roadmap towards enhancing tensile ductility of metal matrix composites," Materials Science and Engineering: A, vol. 648, pp. 92-103, 2015.

[9] S. Sajjadi, H. Ezatpour, and H. Beygi, "Microstructure and mechanical properties of Al–Al 2 O 3 micro and nano composites fabricated by stir casting," Materials Science and Engineering: A, vol. 528, pp. 8765-8771, 2011.

[10] M. Mohammadpour, R. A. Khosroshahi, R. T. Mousavian, and D. Brabazon, "Effect of interfacial-active elements addition on the incorporation of micron-sized SiC particles in molten pure aluminium," Ceramics International, vol. 40, pp. 8323-8332, 2014.

[11] S. K. Selvaraj, M. K. Nagarajan, and L. A. Kumaraswamidhas, "An investigation of abrasive and erosion behaviour of AA 2618 reinforced with Si 3 N 4, AlN and ZrB 2 in situ composites by using optimization techniques," Archives of Civil and Mechanical Engineering, vol. 17, pp. 43-54, 2017.

[12] R. T. Mousavian, R. A. Khosroshahi, S. Yazdani, D. Brabazon, and A. Boostani, "Fabrication of aluminium matrix composites reinforced with nano-to micrometer-sized SiC particles," Materials & Design, vol. 89, pp. 58-70, 2016.

[13] R. Harichandran and N. Selvakumar, "Effect of nano/micro B 4 C particles on the mechanical properties of aluminium metal matrix composites fabricated by ultrasonic cavitation-assisted solidification process," Archives of Civil and Mechanical Engineering, vol. 16, pp. 147-158, 2016

[14] R. T. Mousavian, R. A. Khosroshahi, S. Yazdani, and D. Brabazon, "Manufacturing of cast A356 matrix composite reinforced with nano-to micrometer-sized SiC particles," Rare Metals, pp. 1-9.

[15] R. Raj and D. G. Thakur, "Qualitative and quantitative assessment of microstructure in Al-B 4 C metal matrix composite processed by modified stir casting technique," Archives of Civil and Mechanical Engineering, vol. 16 ,pp. 949-960, 2016.

[16] F. Chen, Z. Chen, F. Mao, T. Wang, and Z. Cao, "TiB 2 reinforced aluminium based in situ composites fabricated by stir casting," Materials Science and Engineering: A, vol. 625, pp. 357-368, 2015.

[17] K. Woo and H. Huo, "Effect of high energy ball milling on displacement reaction and sintering of Al–Mg/SiO2 composite powders," Metals and Materials International, vol. 12, pp. 45-50, 2006.

[18] S. C. Tjong and Z. Ma, "Microstructural and mechanical characteristics of in situ metal matrix composites," Materials Science and Engineering: R: Reports, vol. 29, pp. 49-113, 2000.

[19] K. Gawdzińska, L. Chybowski, and W. Przetakiewicz, "Proper matrix-reinforcement bonding in cast metal matrix composites as a factor of their good quality," Archives of Civil and Mechanical Engineering, vol. 16, pp. 553-563, 2016.

[20] A. Maleki, B. Niroumand, and M. Meratian, "Effects of processing temperature on in-situ reinforcement formation in Al (Zn)/Al2O3 (ZnO) nanocomposite," Metallurgical and Materials Engineering, vol. 21, pp. 283-291, 2015.

[21] Z. Ma and S. Tjong, "In situ ceramic particle-reinforced aluminium matrix composites fabricated by reaction pressing in the TiO2 (Ti)-Al-B (B2O3) systems," Metallurgical and Materials Transactions A, vol. 28, pp. 1931-1942, 1997.

[22] P. Yu, Z. Mei, and S. Tjong, "Structure, thermal and mechanical properties of in situ Al-based metal matrix composite reinforced with Al 2 O 3 and TiC submicron particles," Materials chemistry and physics, vol. 93, pp. 109-116, 2005.

[23] B. Daniel and V. Murthy, "Directed melt oxidation and nitridation of aluminium alloys: a comparison," Materials & Design, vol. 16, pp. 155-161, 1995.

[24] V. Murthy and B. Rao, "Microstructural development in the directed melt-oxidized (DIMOX) Al-Mg-Si alloys," Journal of materials science, vol. 30, pp. 3091-3097, 1995.

[25] O. Salas, H. Ni, V. Jayaram, K. Vlach, C. Levi, and R. Mehrabian, "Nucleation and growth of Al 2 O 3/metal composites by oxidation of aluminium alloys," Journal of materials research, vol. 6, pp. 1964-1981, 1991.

[26] A. V. Muley, S. Aravindan, and I. Singh, "Nano and hybrid aluminium based metal matrix composites: an overview," Manufacturing Review, vol. 2, p. 15, 2015.

[27] M. Hoseini and M. Meratian, "Tensile properties of in-situ aluminium–alumina composites," Materials letters, vol. 59, pp. 3414-3418, 2005.

[28] G. Chen and G.-X. Sun, "Study on in situ reaction-processed Al–Zn/α-Al 2 O 3 (p) composites," Materials Science and Engineering: A, vol. 244, pp. 291-295, 1998.

[29] M. Kobashi and T. Choh, "Fabrication of particulate composite by in situ oxidation process," Light Met, vol. 42, pp. 138-142, 1992.

[30] P. Yu, C.-J. Deng, N.-G. Ma, and D. H. Ng, "A new method of producing uniformly distributed alumina particles in Al-based metal matrix composite," Materials Letters, vol. 58, pp. 679-682, 2004.
[31] T. Durai, K. Das, and S. Das, "Synthesis and characterization of Al matrix composites reinforced by in situ alumina particulates," Materials Science and Engineering: A, vol. 445, pp. 100-105, 2007.
[32] M. Tavoosi, F. Karimzadeh, and M. Enayati, "Fabrication of Al–Zn/α-Al 2 O 3 nanocomposite by mechanical alloying," Materials Letters, vol. 62, pp. 282-285, 2008.
[33] Z.-J. Huang, B. Yang, H. Cui, and J.-S. Zhang, "Study on the fabrication of Al matrix composites strengthened by combined in-situ alumina particle and in-situ alloying elements," Materials Science and Engineering: A, vol. 351, pp. 15-22, 2003.
[34] T. Fan, D. Zhang, G. Yang, T. Shibayanagi, and M. Naka, "Fabrication of in situ Al 2 O 3/Al composite via remelting," Journal of Materials Processing Technology, vol. 142, pp. 556-561, 2003.
[35] S. Shibli, F. Chacko, and C. Divya, "Al 2 O 3–ZrO 2 mixed oxide composite incorporated aluminium rich zinc coatings for high wear resistance," Corrosion Science, vol. 52, pp. 518-525, 2010.
[36] N. Yoshikawa, Y. Watanabe, Z. Veloza, A. Kikuchi, and S. Taniguchi, "Microstructure-Process-Property Realationship in Al/Al2O3 Composites Fabricated by Reaction between SiO2 and Molten Al," in Key Engineering Materials, 1999, pp. 311-314.
[37] H. Zhu, H. Wang, L. Ge, W. Xu, and Y. Yuan, "Study of the microstructure and mechanical properties of composites fabricated by the reaction method in an Al–TiO 2–B 2 O 3 system," Materials Science and Engineering: A, vol. 478, pp. 87-92, 2008.
[38] B. Yang, M. Sun, G. Gan, C. Xu, Z. Huang, H. Zhang, et al., "In situ Al 2 O 3 particle-reinforced Al and Cu matrix composites synthesized by displacement reactions," Journal of Alloys and Compounds, vol. 494, pp. 261-265, 2010.
[39] M. Mohammadpour, R. A. Khosroshahi, R. T. Mousavian, and D. Brabazon, "A novel method for incorporation of micron-sized SiC particles into molten pure aluminium utilizing a Co coating," Metallurgical and Materials Transactions B, vol. 46, pp. 12-19, 2015.
[40] R. T. Mousavian, S. Damadi, R. A. Khosroshahi, D. Brabazon, and M. Mohammadpour, "A comparison study of applying metallic coating on SiC particles for manufacturing of cast aluminium matrix composites," The International Journal of Advanced Manufacturing Technology, vol. 81, pp. 433-444, 2015.
[41] S. Soltani, R. A. Khosroshahi, R. T. Mousavian, Z.-Y. Jiang, A. F. Boostani, and D. Brabazon, "Stir casting process for manufacture of Al–SiC composites," Rare Metals, pp. 1-10, 2015.
[42] R. T. Mousavian, S. Sharafi, and M. Shariat, "Microwave-assisted combustion synthesis in a mechanically activated Al–TiO 2–H 3 BO 3 system," International Journal of Refractory Metals and Hard Materials, vol. 29, pp. 281-288, 2011.
[43] R. T. Mousavian, S. Sharafi, M. Roshan, and M. Shariat, "Effect of mechanical activation of reagents' mixture on the high-temperature synthesis of Al2O3–TiB2 composite powder," Journal of thermal analysis and calorimetry, vol. 104, pp. 1063-1070, 2011.
[44] R. T. Mousavian, N. Azizi, Z. Jiang, and A. F. Boostani, "Effect of Fe2O3 as an accelerator on the reaction mechanism of Al–TiO2 nanothermite system," Journal of Thermal Analysis and Calorimetry, vol. 117, pp. 711-719, 2014.
[45] N. B. Khosroshahi, R. T. Mousavian, R. A. Khosroshahi, and D. Brabazon, "Mechanical properties of rolled A356 based composites reinforced by Cu-coated bimodal ceramic particles," Mater Des, vol. 83, p. 678, 2015.
[46] R. Kheirifard, N. B. Khosroshahi, R. A. Khosroshahi, R. T. Mousavian, and D. Brabazon, "Fabrication of A356-based rolled composites reinforced by Ni–P-coated bimodal ceramic particles," Proceedings of the Institution of Mechanical Engineers, Part L: Journal of Materials Design and Applications, p. 1464420716649631, 2016.
[47] H. Wang, G. Li, Y. Zhao, and G. Chen, "In situ fabrication and microstructure of Al 2 O 3 particles reinforced aluminium matrix composites," Materials Science and Engineering: A, vol. 527, pp. 2881-2885, 2010.
[48] M. Hoseini and M. Meratian, "Fabrication of in situ aluminium–alumina composite with glass powder," Journal of Alloys and compounds, vol. 471, pp. 378-382, 2009.